GEOFIZIKA VOL. 22 2005

Original scientific paper
UDC 551.515.4

The causes of supercell development with tornadogenesis on 30th August 2003 – A case study

Ivana Stiperski

Meteorological and Hydrological Service, Zagreb, Croatia

Received 22 December 2004, in final form 14 July 2005

A supercell storm with tornadogenesis in the afternoon hours of the 30th August 2003 in NW Croatia is studied. As was seen from radar and satellite material the cell developed in Slovenia and crossed into Croatia, where interacting with favorable wind patterns (indicated by high *SREH* and vertical wind shear) it evolved into a supercell. Macroscale forcing was found to be lacking. On the other hand, the pattern, characterized by a pronounced thermal ridge and a baroclinic boundary associated with it, was favorable for supercell generation as has been seen in several studies in the USA. Mesoscale forcing was also enhanced by the existence of the jet stream and outflow boundaries from previous convection associated with a night-time cold front passage. Several severe storm and stability indices were tested for this case and it has been found that they generally did not correspond to the severity of the convection that took place.

Keywords: supercell, baroclinic boundary

1. Introduction

Supercells are steady state rotating convective storms forming in highly sheared environments. They are defined as cells possessing a mesocyclone or vertical vorticity of the order 10^{-2} s^{-1} lasting for tens of minutes (Moller et al., 1994) and displaying deviant motion compared to the mean mid-level wind. Severe weather they are usually associated with includes flash flooding, large hail, severe wind events as well as tornadoes. Although tornadoes do not form exclusively in supercells, those which do, tend to be major ones (Doswell and Burgess, 1993; Doswell, 1996).

Many idealized numerical simulations and field studies have given insight into most of the supercell dynamics (*e.g.* Klemp and Wilhelmson, 1978; Rotunno and Klemp, 1985; Ziegler et al., 2001; Markowski et al., 2002; Markowski et al., 2003). Still some physical processes, especially those governing tornadogenesis, are as yet not well understood. In the meantime, particular interest has been given to studying mesoscale mechanisms, mainly

different types of mesoscale boundaries that are conducive to supercell and tornado development (*e.g.* Maddox et al., 1980; Wilson and Schreiber, 1986; Brooks et al., 1994; Rasmussen et al., 2000).

In this paper a study of a supercell is presented. The objective was to 1) determine the cause of its development and 2) test in European synoptic conditions the applicability and effectiveness of several stability and severe storm indices in a supercell case lacking macroscale forcing. A short overview of supercell environments is given in Section 2. Data used and definitions of indices and other parameters calculated is given in Section 3. A case study of a supercell with reported tornadogenesis on the 30th August 2003 together with results is presented in Section 4. Discussion and conclusion of the results obtained are given in Section 5.

2. Supercell environments

Supercells begin their life cycle as ordinary cells. Due to interaction with environmental vertical wind shear they acquire rotation and evolve into supercells. In their mature stage they consist of a strong usually cyclonically rotating updraft forming the mid-level mesocyclone, and an anticyclonically rotating downdraft on the forward flank of the storm. The evaporatively cooled air from the downdraft forms a pool of cold air beneath the storm, the leading edge of which is known as the gust front. It is a source of lifting as well as vorticity that feeds the mesocyclone.

There are two ways of vorticity generation in supercells: a) tilting and stretching of horizontal vorticity inherent in the environmental shear and b) tilting and stretching of baroclinically generated vorticity on the gust front (Klemp and Rotunno, 1983). The former is responsible for mid-level mesocyclogenesis, while the later is instrumental for low-level mesocyclogenesis. When low-level vorticity production on the gust front (low-level mesocyclone) becomes greater than mid-level vorticity (mid-level mesocyclone) another cyclonically rotating downdraft at the rear flank of the storm is induced. This is the collapse phase of the supercell life cycle in which tornadogenesis can take place (Klemp, 1987). Detailed study of the same exceeds the scope of this paper.

Although supercells form in a rather broad range of *CAPE* (Convective Available Potential Energy) values, extending from few hundred to several thousand J kg^{-1} (*e.g.* Lopez et al., 2001), the crucial feature for their formation and sustenance is vorticity inherent in the environmental shear. Supercell forecasts therefore consist of diagnosing and forecasting environments with wind patterns and thermodynamic conditions supportive of severe convection inside a broader region supportive of convection in general. Those environments are for the United States climatologically mostly found to be warm advection cases connected with quasistationary or warm frontal boundaries.

The typical vertical wind pattern forms a cyclonically curved hodograph with a large loop, almost forming a circle, at low levels showing favorable advective processes (Weisman and Rotunno, 2000). Supercell climatology in Croatia has not been done yet.

2.1. Mesoscale boundaries

It has been documented that supercells interact with baroclinic (also known as thermal) boundaries in a way that enhances their rotation. A typical mesoscale pattern associated with such baroclinic boundaries has been proposed by Maddox et al. (1980) shown on Fig. 1.

Point A is situated within a warm dry air mass with only slight wind shear. Point B inside a hot, moist, unstable air mass exhibits significant veering. In point C situated inside a cool, moist, stable air mass (produced by previous thunderstorm outflow) winds veer slowly with height until the transition takes place into a warmer air mass above, upon which a more pronounced veering occurs. Maddox et al. showed that moisture convergence and cyclonic vorticity at low-levels tend to obtain maximum values across a narrow mixing zone (between points B and C). This is usually the place of supercell occurrence. Following Maddox et al., Rasmussen et al. (2000) investigated several severe tornado events, and verified that cells crossing such a baroclinic boundary show enhancement of low level rotation, producing strong and violent tornadoes. Those that do not cross the boundary or move into the cool air mass develop slower than those crossing the boundary and form only weak tornadoes.

The reason for low level mesocyclone and updraft intensification upon crossing the boundary lies in a) vertical vorticity production on the boundary, b) tilting of horizontal vorticity in the direction of the flow, as well as c) con-

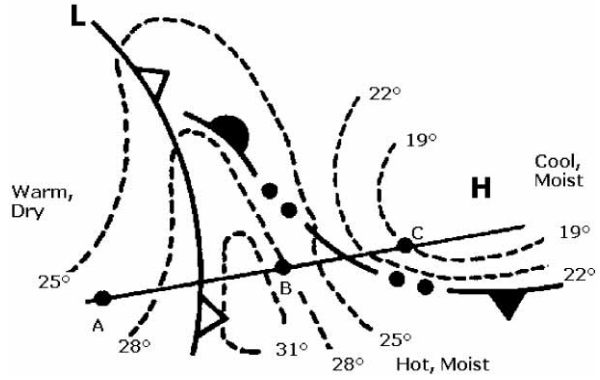

Figure 1. Typical mesoscale surface pattern supportive of supercell development. Broken line represents isotherms in degrees Celsius. The dotted front line indicates the position of the baroclinic boundary (adopted from Maddox et al., 1980).

vergence (stretching) associated with the boundary. Strong low-level thermal gradients across the boundary act in such a way as to enhance the veering of the wind in case of warm advection, while decreasing it on the cool side of the boundary where cold advection prevails (Rasmussen et al., 2000).

2.2. Supercell diagnostics and forecasts

It is important to note that forecasting supercells is not equivalent to forecasting tornadoes. There are many parameters governing tornadogenesis, however covering all the methods of tornado prediction is beyond the scope of this study. Still we may note that an important factor in tornadogenesis is the availability of dry air in the downdraft entrainment region for low-level baroclinic vorticity production to occur (Johns and Doswell, 1992).

Diagnostic tools for the estimation of supercells potential include stability and moisture convergence assessments, as well as recognition of favorable wind shear patterns. Potential for mid-level mesocyclone, and therefore supercell development, can be assessed by means of storm relative helicity (*SREH*). *SREH* is a measure of correlation between vertical vorticity and vertical velocity as defined in (6). Thus in the cases when both vertical velocity and vertical vorticity have the same sign and large values *SREH* will be high and positive. It is a good diagnostic of supercell potential, as high values of positive vertical vorticity and vertical velocity (high *SREH*) in lower levels lead to strong updraft and mesocyclone development (Bluestein, 1993). Low--level mesocyclogenesis is, on the other hand, very sensitive to the balance

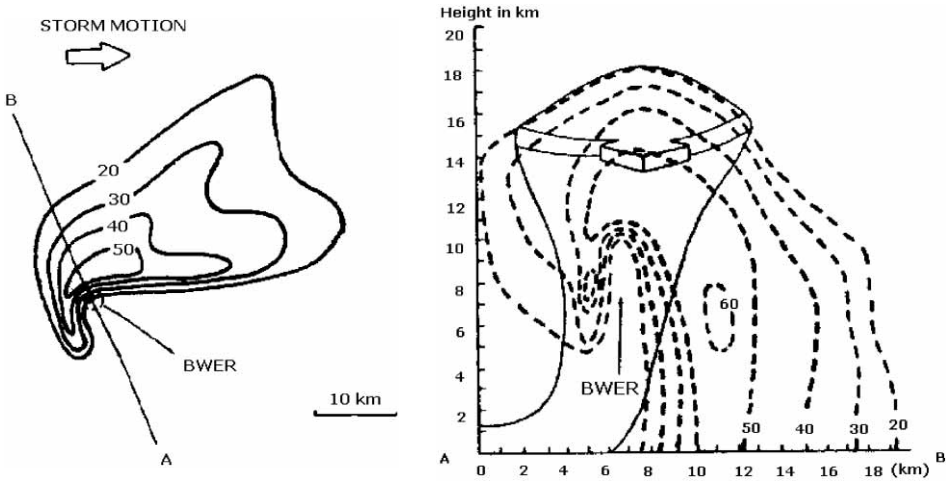

Figure 2. Schematic diagram of a supercell as seen on radar. a) Horizontal cross-section (PPI). Solid lines are radar reflectivity contours in dBz. b) Vertical cross-section (RHI). Dashed lines are radar reflectivity in dBz, while solid lines show the updraft position. Pronounced BWER is indicated (adopted from Bluestein, 1993).

between the strength of mid-level storm-relative winds and the mid-level mesocyclone (a function of *SREH*). The reason is that both act to horizontally redistribute precipitation about the updraft and thus influence baroclinic generation of low-level vorticity and eventually tornadogenesis (Kerr and Darkow, 1996).

Real time supercell detection and recognition, once convection is initiated, is greatly facilitated by the use of Doppler Radars. Characteristic features of a supercell as seen on radar are the existence of a persistent mesocyclone, deviant motion compared to the mean wind, and BWER (Bounded Weak Echo Region). BWER is the updraft region of the supercell (Moller et al., 1994) and is seen on the radar image as a bounded area of weak echoes (Fig. 2).

3. Storm parameters

3.1. Stability indices

There are many stability indices defined for atmospheric thermodynamic structure evaluation. In this study the following were used: *K* index, Totals-Totals index and Showalter index.

The indices were computed according to their standard definitions (Bluestein, 1993).

K index $$K = T_{850} - T_{500} + T_{d850} - (T_{700} - T_{d700}) \quad (1)$$

Totals-Totals index $$TT = T_{850} + T_{d850} - 2T_{500} \quad (2)$$

Showalter index $$SI = T_{500} - T'_{850-500} \quad (3)$$

where T_{850}, T_{700} and T_{500} are environmental temperatures at 850, 700 and 500 hPa respectively with the subscript $_{\mathrm{d}}$ indicating dew point temperature. $T'_{850-500}$ represents the temperature an air parcel has after being lifted from 850 hPa dry-adiabatically to LCL and then moist-adiabatically to 500 hPa. *K* index values between 31–35 °C are taken to indicate scattered, while those greater than 36 give a potential for numerous thunderstorms (George, 1960). The correspondent Totals-Totals index values for scattered to numerous thunderstorms is 52–55 °C (Miller, 1972). When Showalter index values are below 0 the likelihood of showers and thunderstorms is increased (Showalter, 1953).

3.2. Severe thunderstorm indices

Apart from evaluating the statical stability of the atmosphere severe thunderstorm indices also take into account the dynamical factors essential in supercell formation: such as wind speed and directional variations. Bulk

Richardson number, measuring the influence of instability (*CAPE*) versus the square of mean wind in the lowest 6 km layer, is often used as an indicator of severe thunderstorm type, distinguishing between multicellular and supercellular storms (Bluestein, 1993).

$$R_B = \frac{CAPE}{\frac{1}{2}(\overline{u}^2 + \overline{v}^2)} \tag{4}$$

R_B values falling within the 10–40 limit are generally thought to be indicative of supercells (Moller et al., 1994). Severe Weather Threat Index (*SWEAT*) is defined as

$$SWEAT = 12(T_{d850}) + 20(TT - 49) + 2(\vec{v}_{850}) + (\vec{v}_{500}) + 125(\sin(d_{500} - d_{850}) + 0.2) \tag{5}$$

where *TT* is Totals-Totals index, $\vec{v}$ and d with a subscript denote wind speed and direction respectively, at the said isobar level. Values greater than 200 are usually taken to indicate supercell formation potential while those greater than 400 are associated with tornadoes (Miller, 1972). Storm Relative Environmental Helicity (*SREH*) is a measure of the influence of wind field patterns on the supercell formation. It is defined in the following way

$$SREH = -\int_0^h \vec{k} \cdot (\vec{v} - \vec{c}) \times \frac{\partial \vec{v}}{\partial z} dz \tag{6}$$

where $\vec{k}$ is the vertical unit-vector, $\vec{v}$ denotes the environmental wind vector and $\vec{c}$ is the storm motion vector. Value of h is usually 3 km, but recent studies have shown that *SREH* in the 1 km layer might be a better forecasting tool in distinguishing between tornadic and non-tornadic supercells (Rasmussen, 2003). Values greater than 150 m^2s^{-2} are favorable for tornado development (Kerr and Darkow, 1996). Energy-Helicity Index (*EHI*) was shown to be a better forecast parameter than either shear or *CAPE* alone (Rasmussen, 2003). It is defined as a product of *CAPE* and *SREH*

$$EHI = CAPE \cdot SREH \,/\, 160\,000 \tag{7}$$

Values greater than 1 are used as being indicative of supercell development, but the study by Gaya (1997) showed that only 3 out of 10 tornado cases in Balearic Islands had *EHI* values higher than 1, indicating that this threshold might be unrepresentative in Mediterranean conditions. The other reference values might also be unsuitable for supercell prediction in Europe.

4. Case study

4.1. Data

In this case study standard forecasting and diagnostic material available at Croatian Meteorological and Hydrological Service was used. Diagnostic weather data consisted of Zagreb sounding, satellite and radar images as well as various synoptic charts. Products of hydrostatic numerical mesoscale model ALADIN (Aire Limitee Adaptiation Dynamique et Developpement International) in form of horizontal and vertical (pseudoTEMP) variable fields were also used. The model resolution is 12.2 km and the model has 37 levels. Different stability indices, helicity and wind shear were calculated from pseudoTEMPs, alongside Energy-Helicity Index (*EHI*), Convective Available Potential Energy (*CAPE*) and Bulk-Richardson Number (R_B) calculated from Zagreb sounding data (*i.e.* Fig 9).

Still caution should be taken when dealing with forecast material in cases of severe weather. Operational models tend to be unrepresentative and

Figure 3. Reference map of Croatia.

cannot resolve well the small scale features of the low level environment, which are the paramount feature of supercell formation and particularly tornadogenesis.

4.2. Synoptic situation

During the early morning hours of 30th August 2003 Croatia was under the influence of a cold front passage associated with severe weather. The cold front was also responsible for secondary cyclogenesis in northern Italy, which was the main synoptic feature in the afternoon hours. A warm front attached to the system was extending over the Alps (Fig. 4a). The existence of jet stream over Croatia was visible on 300 hPa chart at 00 UTC (Fig. 4b), while its existence in the afternoon hours could be retrieved from the 12 UTC Zagreb sounding.

4.3. Satellite and Radar data

The storm developed as an ordinary convective cell over central Slovenia in late morning hours of 30th August 2003, becoming visible on satellite imagery around 12 UTC (Fig. 5). Images from the radar station Trema near Križevci showed that the cell entered Croatia in the vicinity of Krapina (for

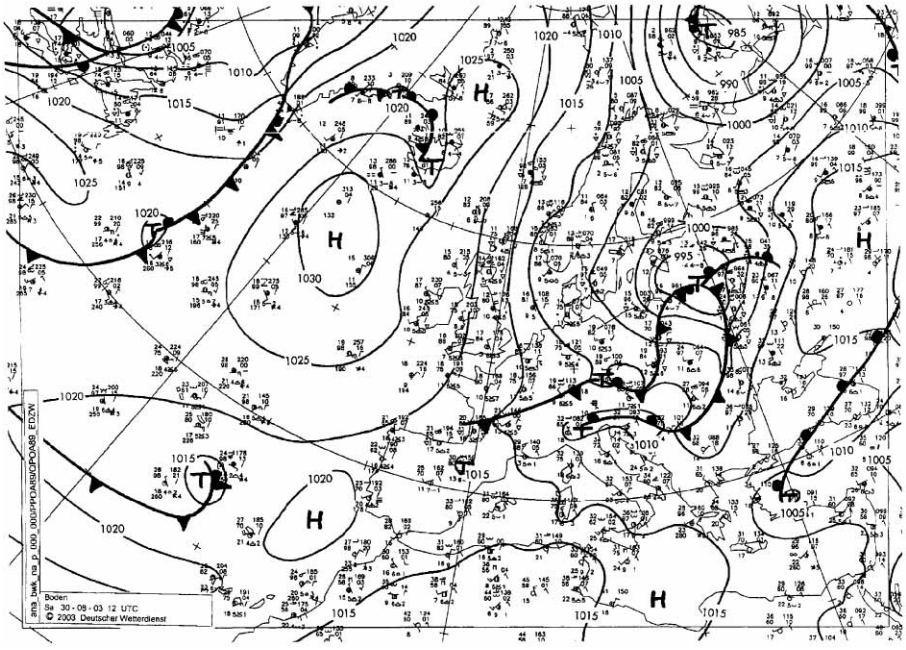

Figure 4 a. Ground level synoptic chart on 30th August 2003 at 12 UTC.

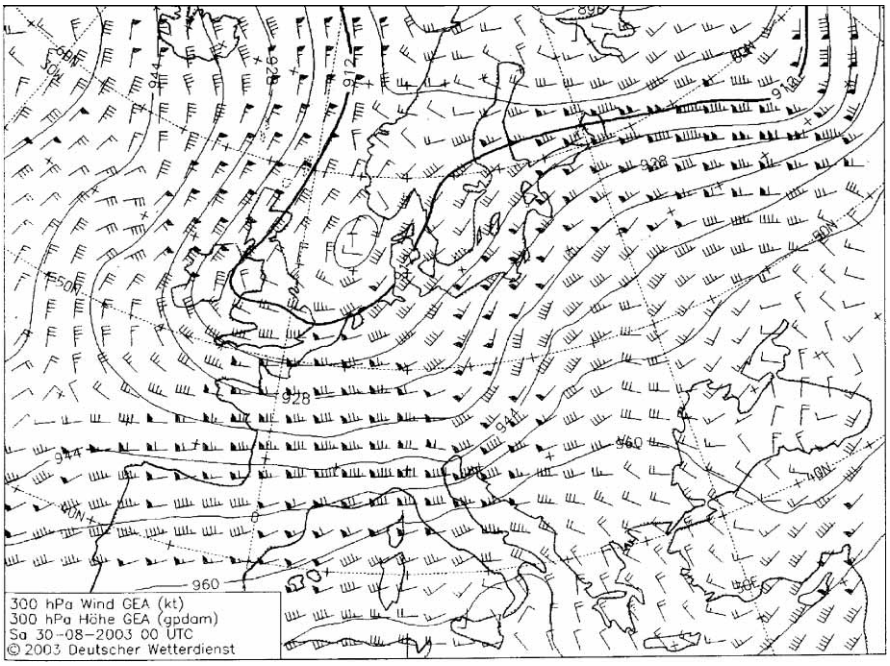

Figure 4 b. Upper level synoptic chart (300 hPa) on 30th August 2003 at 00 UTC. Solid lines are geopotential height in gpdam. Wind is indicated by arrows, wind speed given in knots.

reference see Fig. 3) at 12.26 UTC. At 13.14 UTC certain supercell characteristics could be discerned, such as a pronounced region of strong updraft and WER (Weak Echo Region) as seen in Fig. 6a, making it possible to conclude that the cell evolved into a supercell around that time. In Fig. 6 b and c, a pronounced BWER can be seen, with mesocyclone advecting precipitation around the updraft core thus producing a region of closed reflectivity around the updraft, visible also on the vertical cross-section at 13.30 UTC (Fig. 6d). The supercell reached its maximum intensity both in reflectivity (65–70 dBZ) and in the damage produced around 13.33 UTC over sv. Petar Orehovec. A slowdown in its propagation velocity lasting approximately 15 minutes was observed during that time. A hook echo at the southern most part of the cell could be noted in the radar images of the same period (Fig. 6e, f). The supercell was in the tornadic phase. The observer at Bilogora radar station reported seeing a funnel cloud. However the damage (roof pealed off a local school building) and observations are consistent with only a weak tornado formation, estimated to be of F1 intensity of the Fujita Scale (Fujita, 1971). Still due to the lack of quality Doppler radar images it was not possible to determine quantitatively the existence of mesocyclone either at mid- or at low-levels. After reaching its maximum intensity the storm continued in the direction of Đurđevac maintaining BWER both in the horizontal and in the vertical, and finally left

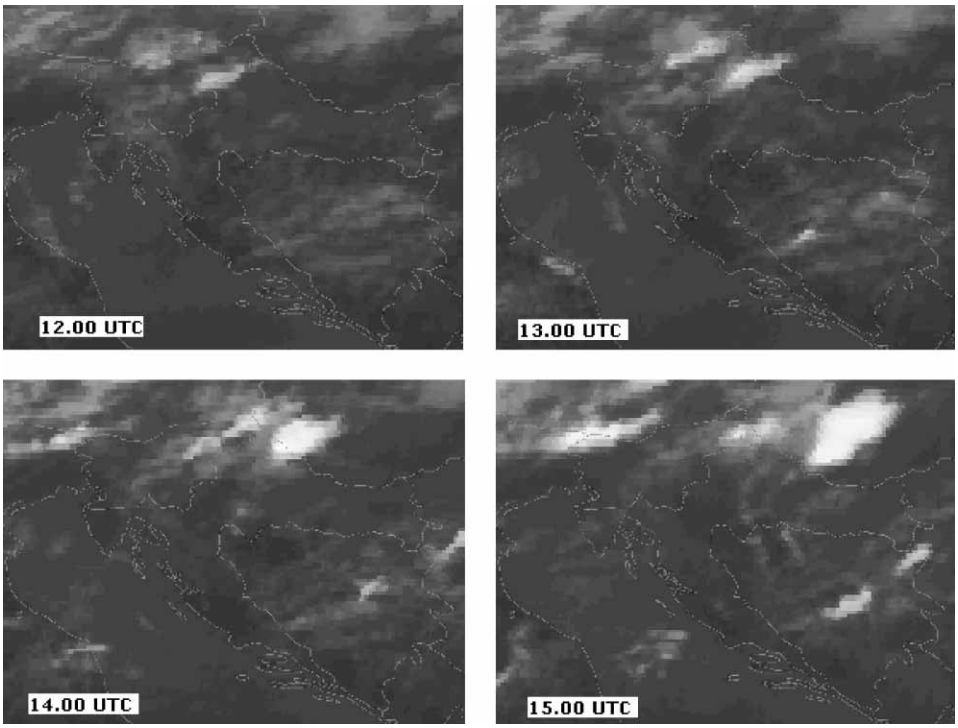

Figure 5. Infrared METEOSAT-7 satellite images for 30th August 2003.

Croatia at approximately 15 UTC proceeding into Hungary. During its passage through Croatia the mean supercell propagation velocity was approximately 16 m/s in the direction of WNW as calculated from the radar images.

4.4. Mesoscale situation

On the vertical time cross-sections (High Resolution Isentropic Diagnostic, HRID), passage of a shallow mesoscale warm front (baroclinic boundary) in northern Croatia (*i.e.* Križevci) was forecasted in the late morning hours of 30th August 2003 (Fig. 7). It was indicated by downward sloping lines of constant equivalent potential temperature as well as by the existence of weak baroclinicity, the atmosphere being convectively unstable.

As seen in the measured temperature surface field at 12 and 15 UTC (Fig. 8) a pronounced stationary thermal ridge was the main mesoscale feature in the domain of the storm. It shows some similarities with mesoscale pattern proposed by Maddox et al. (1980). However contrary to the Maddox model the southern region of the thermal ridge was not just warm but also dry, and the central part with even higher temperatures had also very low humidity (less than 40 %) as seen in Figures 8 and 9. From the measure-

ments it is clear that the position of the baroclinic boundary was in the northern part of Croatia in the WSW-ENE direction. Prognostic charts show that this region was under the influence of pronounced moisture convergence (Fig. 10) as well as convergence in the wind field and positive vertical velocities (not shown). Surface moisture convergence (*MOCON*) was calculated here in the following way:

$$MOCON = -r_{2m}\nabla(\vec{v}_{10m}) - \vec{v}_{10m} \cdot \vec{\nabla} r_{2m} \tag{8}$$

where r_{2m} is relative humidity at 2m and $\vec{v}_{10m}$ is the wind at 10 m.

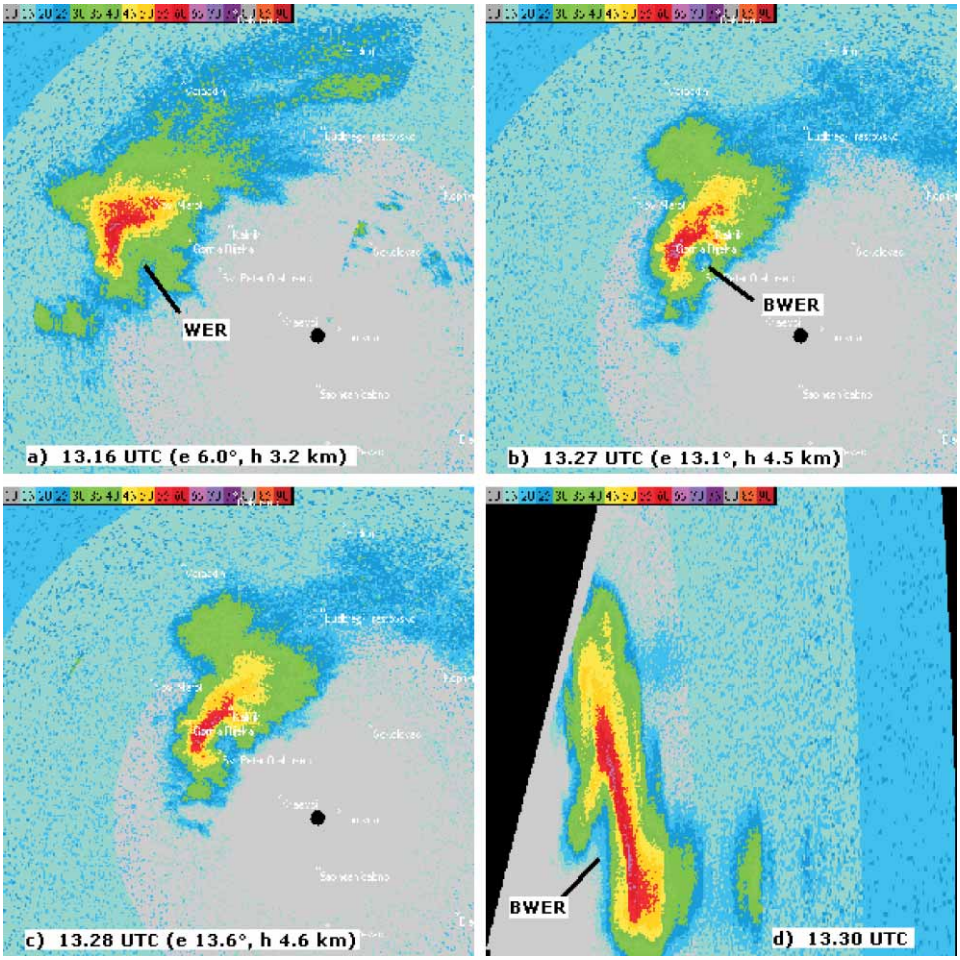

Figure 6. CAPPI (a–c, e–f) and RHI (d) radar image cross-sections taken from radar center Trema near Križevaci on 30th August 2003. Here e is the elevation angle, h the mean height of the cloud at the observed level.

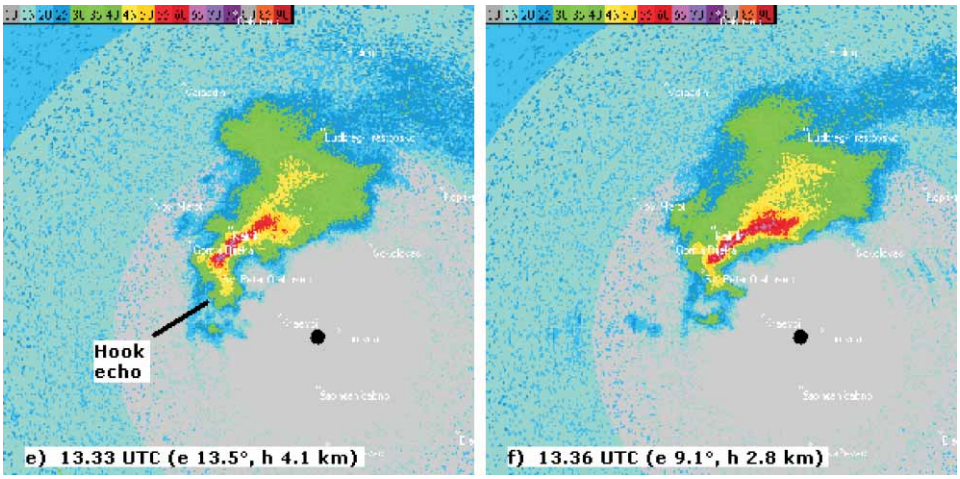

Figure 6. continued.

It can be noted that compared to 12 UTC the area under the influence of moisture convergence at 15 UTC had increased and north-western Croatia was experiencing weak convergence.

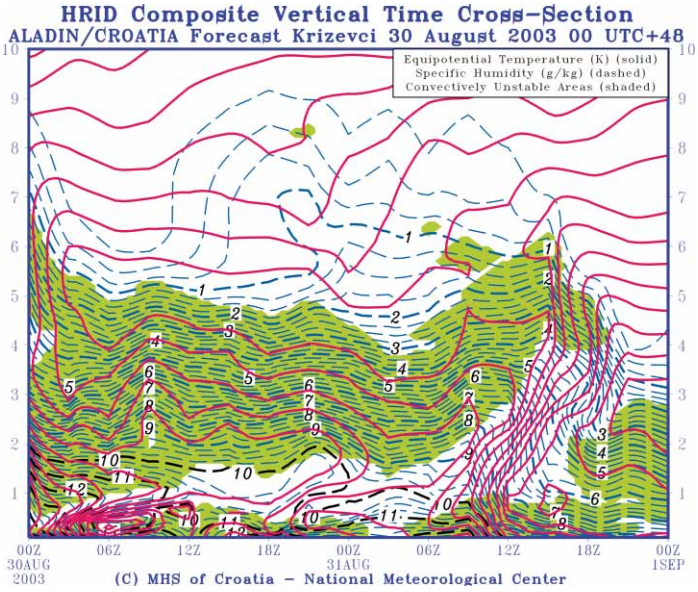

Figure 7. Composite vertical time cross-section (HRID) 48 hour forecast based on the 00 UTC run of ALADIN model on 30th August 2003 for Križevci. In the graph equipotential temperature (solid lines), specific humidity (dashed) and convectively unstable areas (shaded) are plotted.

During it's most intense phase the storm's position was on the cool side of what is presumed to be the position of the baroclinic boundary. Thus it shows similarities with the analysis of several supercell weak tornado outbreaks along a baroclinic boundary in the USA studied by Rasmussen et al. (2000) discussed in the introduction.

Winds at 700 hPa were predominantly from the southwest (SW), while wind field at the surface exhibited a very complex pattern. Northern and northwestern Croatia accordingly experienced winds mostly from northeast (NE), with a jet stream at high levels observed on the synoptic charts. Croatia and Slovenia were both situated within the left exit region of the jet, associated with ascending motion.

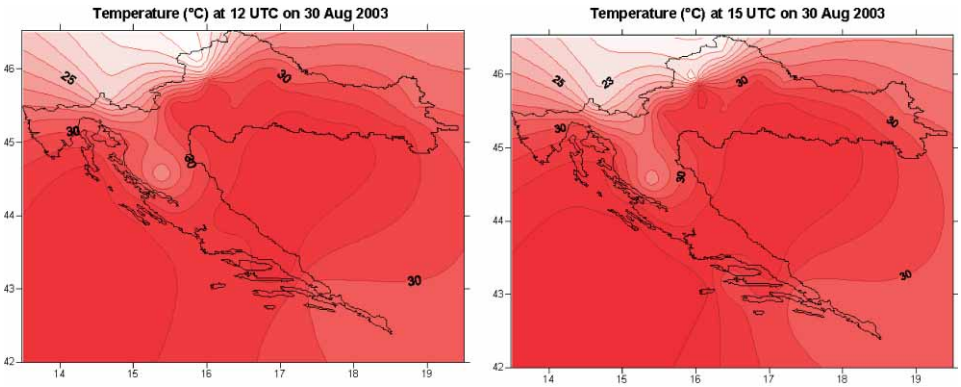

Figure 8. Surface temperature (°C), 12 (left) and 15 (right) UTC analysis on the 30th August 2003. A thermal ridge is visible extending to central Croatia and the large temperature gradient associated with it is visible in the NW Croatia. Isotherms are drawn at a 1 °C interval.

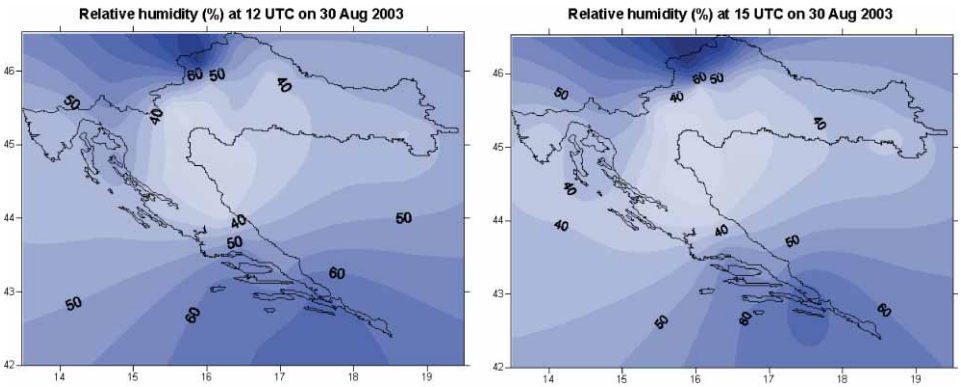

Figure 9. Surface relative humidity (%), 12 (left) and 15 (right) UTC analysis on the 30th August 2003. A large humidity gradient is visible in NW Croatia. Lines of constant relative humidity are drawn at a 10% interval.

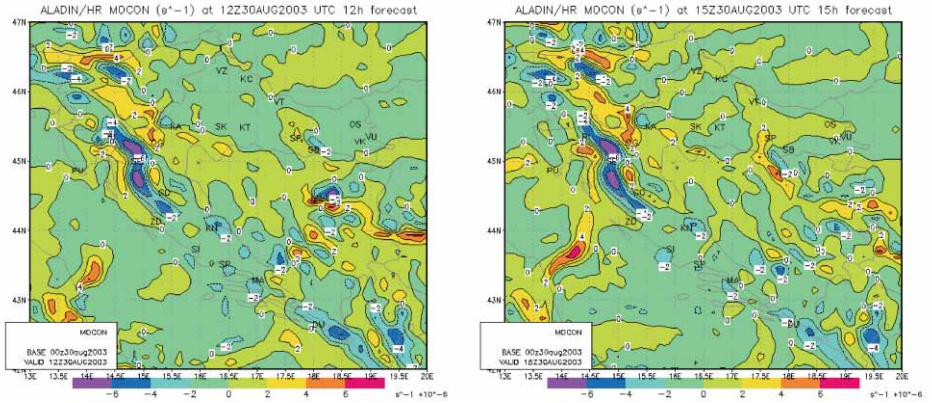

Figure 10. Surface Moisture Convergence (*MOCON*) (s^{-1}) for 12 (left) and 15 (right) UTC, a forecast starting at 00 UTC on 30th August 2003. Central Slovenia and Gorski Kotar in Croatia (see Fig. 3) are under the influence of moisture convergence while northern parts of coastal Croatia are experiencing pronounced moisture divergence.

4.4.1. Zagreb sounding

Zagreb sounding cannot really be considered a proximity sounding (Maddox, 1976) due to large spatial variability of the thermodynamic fields (see Fig. 8 and 9). It is still of relevance since it was the nearest sounding to the actual location of the supercell, Zagreb being situated some 35 km away from the place where the most intensive phase of the cell was recorded. The shape of the sounding was very similar to the Inverted V Miller sounding (Bluestein, 1993) usually characteristic of Low Precipitation supercells and dryline environment (Fig. 11). It was characterized by the absence of significant low level moisture, almost adiabatic environmental lapse rate and a pronounced mid-level humidity minimum. This indicates that the boundary was possibly case of a hybrid front having characteristics of both baroclinic warm front and dryline. On the other hand the cell itself developed in eastern Slovenia which as seen in Fig. 10 suffered no lack of low level moisture due to low level moisture convergence. It can therefore be concluded that the thermodynamic picture of the environment supplied by the sounding was unrepresentative of the air mass in which the storm originally developed, but was representative of the environment into which the storm eventually moved. Thus once the cell entered Croatia the absence of significant low level moisture as well as very dry air at midlevels (700 hPa upward) heightened the potential of strong downdrafts. *CAPE* values calculated from the sounding (823 J kg^{-1}) together with stability indices showed moderate instability (*TT* = 48.2 °C, *SI* = –0.4 °C). Still there was relatively high possibility of severe convection formation in the air mass described by the sounding according to the K index (values of 32.7 °C).

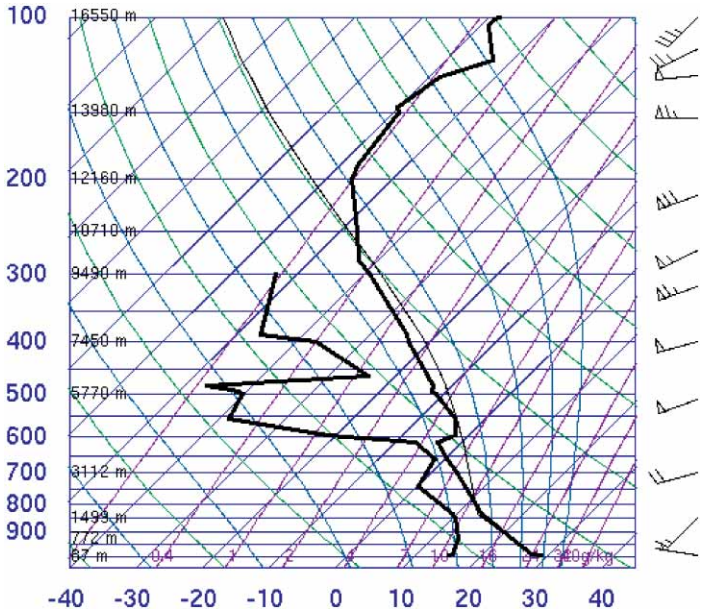

Figure 11. Zagreb sounding on 00 UTC 30th August 2003 skew T-log p graph. The right line is temperature, while the left is dew point temperature. Wind speed is given in knots.

Hodograph curvature was typical of a right-moving supercell with pronounced shear and veering in the first 3 km, in the shape of a semi-circle (Fig. 12). Vertical wind shear in the first 6 km was found to be of moderate intensity (3.3×10^{-3} s^{-1}), with R_B (equal 13) supportive of supercell development. *SREH* was, on the other hand, very low (61 m^{2}s^{-2}). When substituting surface wind values measured in Križevci (the nearest synoptic station to the supercell occurrence) into the Zagreb sounding, one gets a slightly higher *SREH* value of around 80 m^{2}s^{-2}. Still both values are very low compared to the values obtained from the ALADIN model output (compare Fig. 13f) which leads to the question of how well the model represents local wind features. *EHI* values computed from the sounding (0.31 m^{4}s^{-4}) were, due to low *SREH*, below what is usually taken as favorable for supercells. The existence of jet stream noted on synoptic charts at 00 UTC was also observed in the sounding in the layer between 390–146 hPa with the maximum speed of 35.6 m/s at 214 hPa.

4.4.2. Severe Storm Parameter fields

The mesoscale situation changed only little in the time period discussed (12–15 UTC). However severe storm indices showed more pronounced variability. It can generally be noted that stability and severe storm indices computed from the model output didn't correspond to the severity of convection

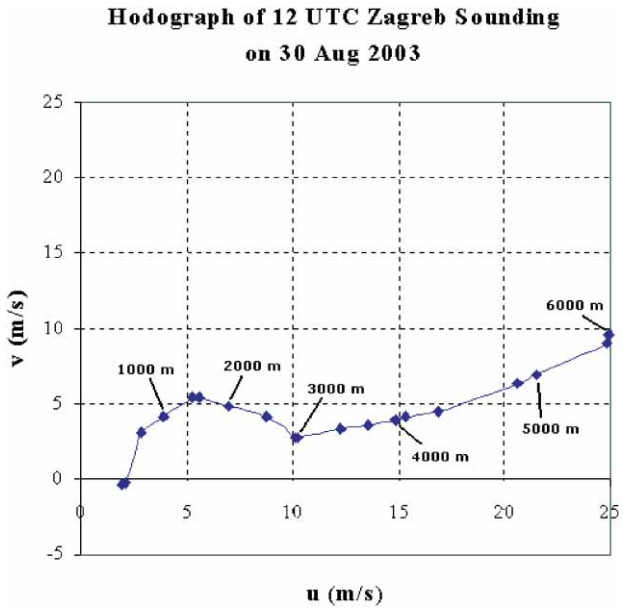

Figure 12. Hodograph retrieved from 30th August 2003 00 UTC Zagreb sounding data.

initiated. The 12 UTC values of Showalter were found to be relatively high (greater than 0 °C) indicating only marginal instability or even stability (Fig. 13). It is thought that the lack of low level moisture in northern Croatia was responsible for unrealistic values. *K*-index and Totals-Totals index on the other hand, indicated a more pronounced instability, although not high enough for severe thunderstorms to be initiated. Vertical wind shear was of moderate intensity (4×10^{-4} s^{-1}) and alongside 0–3 km *SREH* (150 m^{2}s^{-2}) was sufficient for supercell formation to take place, although not high enough to propose a significant tornado threat. *SREH* in the 0–1 km layer (~ 40 m^{2}s^{-2}) was below what is thought to be the threshold for low level mesocyclogenesis. *SWEAT* index values (250–300) showed potential for thunderstorm development but were below tornadogenesis possibility threshold, for USA accepted to be greater than 400. Still compared to values calculated from 12 UTC Zagreb sounding, the model-computed *SWEAT* was unrealistically large the same as *SREH*.

In Fig. 14 the 15 UTC parameter fields are shown. A marginal decline in 0–3 km *SREH* (180 m^{2}s^{-2}), but greater *SWEAT* (300–350) values in the northeast of Croatia (which was at that time the region of interest) were observed, indicating heightened probability of severe thunderstorms. A weak rise in instability could also be noted (*TT* and *SI*) but the values remained short of the severity of convection that was taking place. During the whole period vertical wind shear values remained nearly constant (~ 4×10^{-3} s^{-1}).

5. Conclusion

While synoptic scale forcing mechanisms were lacking, the main mesoscale feature during the time of the storm was a baroclinic boundary in the NW part of Croatia. The environment in which the storm initially developed was rich in moisture and instability while the convergent baroclinic boundary provided lifting essential in convection triggering and subsequent transition into a supercell. Lifting was also facilitated by the existence of the jet stream, whose left exit region was associated with cyclonic vorticity and lifting over Slovenia and Croatia. Across the boundary large temperature (0.3 °C km^{-1}) and humidity (1.2 % km^{-1}) gradients were measured. The buoyancy gradient contributing to streamwise vorticity was of the order 10^{-2} ms^{-1} per kilometer.

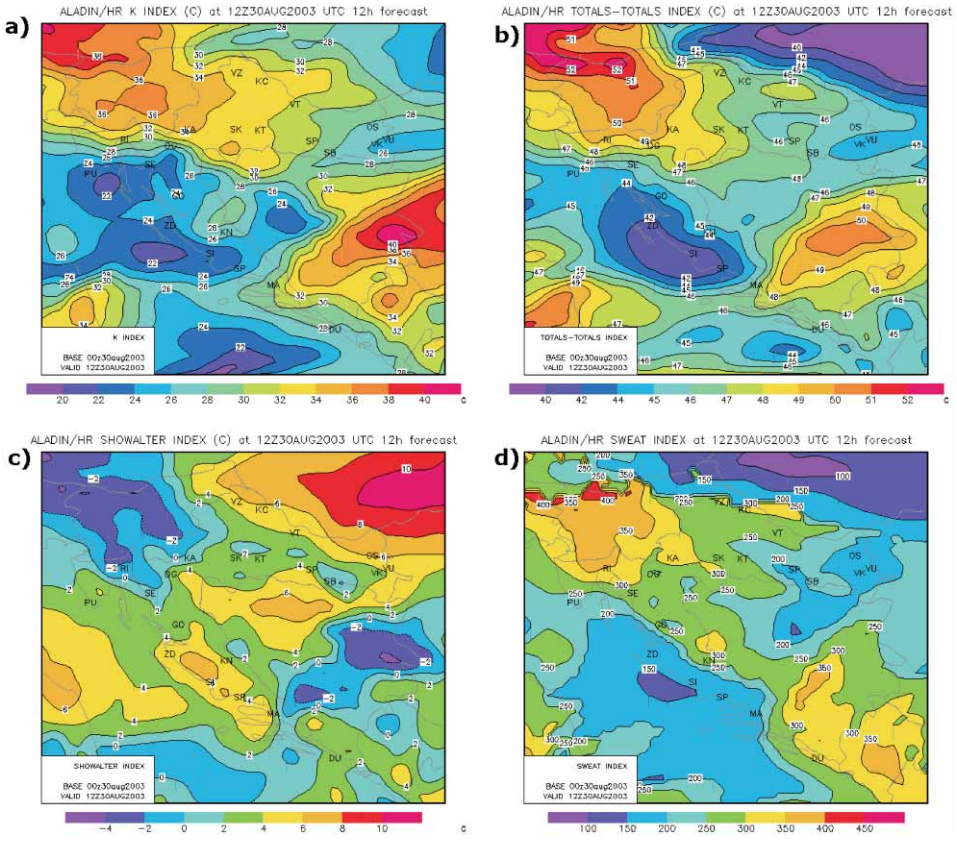

Figure 13. Horizontal variable fields: a) K index, b) Totals-Totals index, c) Showalter index, d) *SWEAT* index, e) *SREH* in 0–1 km layer, f) *SREH* in 0–3 km layer and g) vertical wind shear in 0–6 km layer, at 12 UTC, a forecast starting from 00 UTC on 30th August 2003.

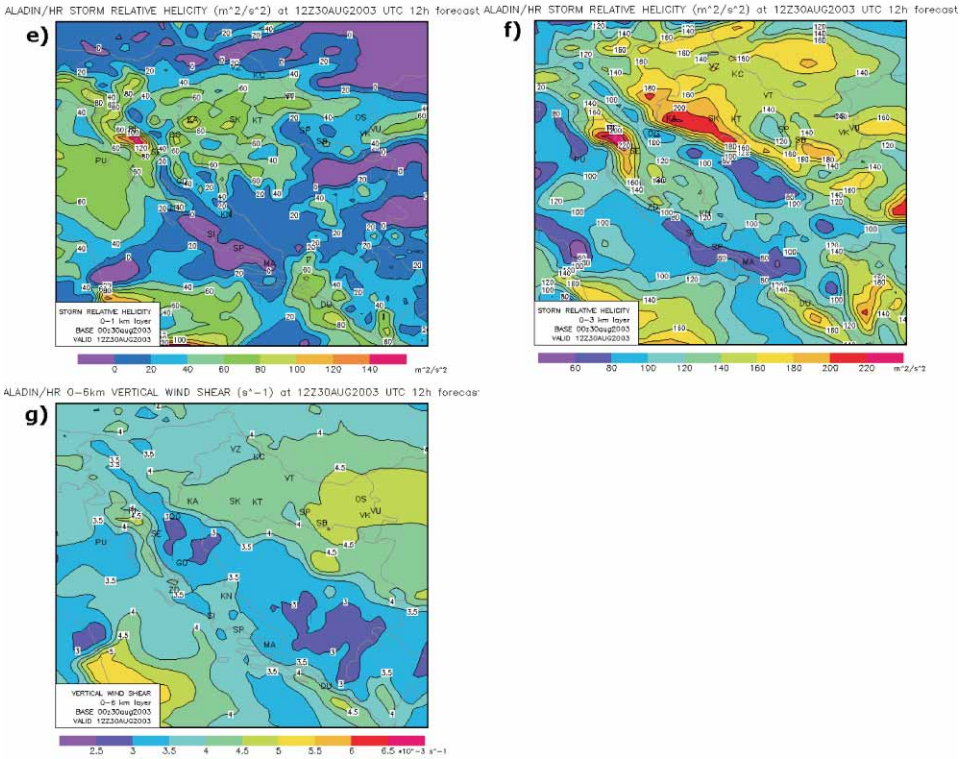

Figure 13. Continued.

The baroclinic boundary showed characteristics of a stationary mesoscale warm front as was observed in the surface analysis, while in the sounding some dryline characteristics were suggested, making it a possible case of a hybrid front. Since the exact position of the boundary could not be determined (due to the lack of quality radar images) it was impossible to establish whether the storm crossed the boundary thus acquiring intensification of low-level rotation, or not. It is plausible to suspect though that no boundary crossing was present, as the storm developed near the tip of the thermal ridge subsequently moving into the cool air mass (Rasmussen, 2000). The damage done was also consistent with only weak tornado of F1 intensity according to Fujita scale.

Our aim was to test the applicability of the model-calculated fields in forecasting the environment conducive to the genesis of the supercell, as well as diagnose what that environment was. Dynamical factors such as vertical wind shear and *SREH* calculated from the model forecast were conducive to supercell development. Still, values retrieved from the sounding were not so pronounced. Also, numerical calculations of different stability and severe

weather indices showed that thermodynamic structure of the atmosphere over north-western Croatia was in fact not very favorable for severe storm formation (*K*, *TT*, *SI*). Among these Showalter index proved least satisfactory but is taken to be unrepresentative in the case studied due to the lack of low-level moisture. *SWEAT* index values indicated supercell development

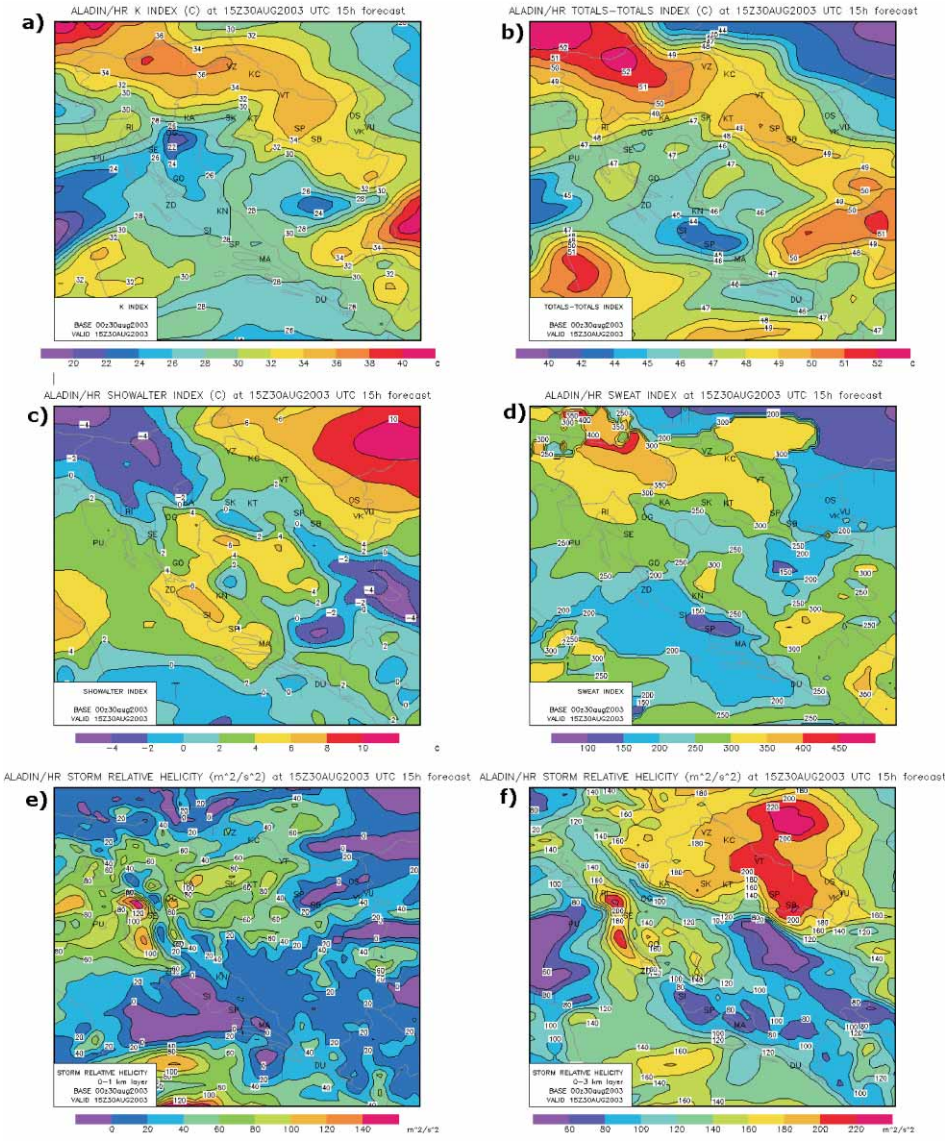

Figure 14. As in Fig. 13 for 15 UTC, forecast starting from 00 UTC on 30th August 2003.

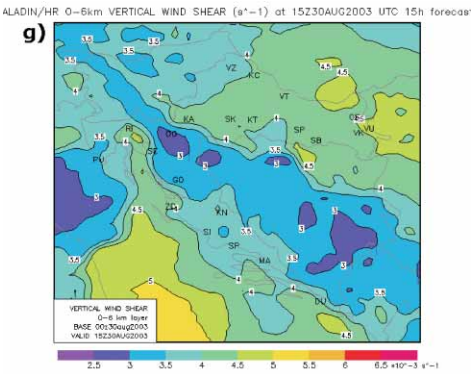

Figure 14. Continued.

possibility but weren't conducive to tornadogenesis. Comparison with Zagreb sounding data shows that the model reproduced the environment relatively well (except for overestimating *SWEAT* index and *SREH* values when compared to Zagreb sounding computed ones), but that the indices themselves were not indicative of the severity of the convection that eventually took place. However one should also be aware of the model limitations in forecast such situations that lack macroscale forcing.

Limitations inherent to indices computations should also be born in mind since the processes they try to quantify are themselves still poorly understood and many aspects are not taken into account (Johns and Doswell, 1992). This makes constructing a reliable forecast tool still very difficult. Another problem arises from the fact that indices validations are usually limited to USA and the issue of applying the same results to geographically and climatologically diverse areas, like Europe still remains. It is therefore essential to determine the environments in which supercells form in Europe and accordingly to determine parameter thresholds valid for those cases. This would in the future include making an extensive supercell and tornado climatology database for specific parts of Europe as has been done for *e.g.* Balearic Islands (Gaya, 1997). Such an undertaking is currently being done through European Severe Weather Database (ESWD).

References

Bluestein, H. B. (1993): *Synoptic-Dynamic Meteorology in Midlatitudes*. Vol II: Observations and Theory of Weather Systems, Oxford University Press, 431–538.

Brooks, H. E. and Doswell III, C. A. (1994): On the Environment of Tornadic and Nontornadic Mesocyclones. *Weather Forecast.*, **9**, 606–617.

Doswell III, C. A. and Burgess, D. W. (1993): Tornadoes and Tornadic storms: A Review of Conceptual Models, The Tornado: Its Structure, Dynamics, Prediction and Hazards. Geophisical Monograph 79, Amer. Geophys. Union, 161–172.

Doswell III, C. A. (1996): What is a Supercell? *18th Conf. Severe Local Storms* (San Francisco, CA). 19–23 February, Amer. Meteorol. Soc., 641 pp.

Fujita, T. T. (1971): Proposed Characterization of Tornadoes and Hurricanes by Area and Intensity. SMRP Research Paper No. 91. University of Chicago, 42 pp.

Gaya, M., Ramis, C., Romero, R., and Doswell III, C. A. (1997): Tornadoes in the Balearic Islands (Spain): Meteorological Setting. *INM/WMO International Symposium on Cyclones and Hazardous Weather in the Mediterranean*, WMO, 525–534.

George, J. J. (1960): *Weather Forecasting for Aeronautics*. Academic Press, New York

Johns, R. H. and Doswell III, C. A. (1992): Severe Local Storm Forecasting. *Weather Forecast.*, **7**, 588–612.

Kerr, B. N. and Darkow, G. L. (1996): Storm-Relative Winds and Helicity in the Tornadic Thunderstrom Environment. *Weather Forecast.*, **11**, 489–505.

Klemp, J. B. and Wilhelmson, R. B. (1978): The Simulations of Three-Dimensional Convective Storm Dynamics. *J. Atmos. Sci.,* **35**, 1070–1096.

Klemp, J. B. and Rotunno, R. (1983): A study of Tornadic Region within Supercell Thunderstorms. *J. Atmos. Sci.,* **40**, 359–377.

Klemp, J. B. (1987): Dynamics of Tornadic Thunderstorms. *Annu. Rev. Fluid Mech.*, 19, 369–402.

Lopez, L, Marcos, J. L., Sanchez, J. L., Castro, A., and Fraile, R. (2001): CAPE Values and Hailstorms on northwestern Spain. *Atmos. Res.*, **56**, 147–160.

Maddox, R. A. (1976): An Evaluation of Tornado Proximity Wind and Stability Data. *Mon. Weather Rev.*, **104**, 133–142.

Maddox, R. A., Hoxit, L. R., and Chappell, C. F. (1980): A study of Tornadic Thunderstorm Interaction with Thermal Boundaries. *Mon. Weather Rev.*, **108**, 322–336.

Markowski, P. M, Straka, J. M., and Rasmussen, E. N. (2002): Direct Surface Thermodynamic Observations within Rear-Flank Downdrafts of Nontornadic and Tornadic Supercells. *Mon. Weather Rev.*, **130**, 1692–1721.

Markowski, P. M, Straka, J. M., and Rasmussen, E. N. (2003): Tornadogenesis Resulting from Transport of Circulation by a Downdraft: Idealized Numerical Simulations. *J. Atmos. Sci.,* **60**, 795–823.

Miller, R. C. (1972): Notes on analysis and severe-storm forecasting procedures of the Air Force Global Weather Central. AWS Tech. Rpt. 200 (rev). Air Weather Service, Scott AFB, IL, 109 pp.

Moller, A. R., Doswell III, C. A., Foster, M. P. and Woodall, G. R. (1994): The Operational Recognition of Supercell Thunderstorm Environments and Storm Structures. *Weather Forecast.*, **9**, 327–347.

Rasmussen, E. N., Richardson, S., Straka, J. M., Markowski, P., and Blanchard, D. O. (2000): The Association of Significant Tornadoes with a Baroclinic Boundary on 2 June 1995. *Mon. Weather Rev.*, **128**, 174–191.

Rasmussen, E. N. (2003): Refined Supercell and Tornado Forecast Parameters. *Weather Forecast.*, **18**, 530–535.

Rotunno, R. and Klemp, J. B. (1985): On the Rotation and Propagation of Simulated Supercell Thunderstorms. *J. Atmos. Sci.,* **42**, 271–291.

Showalter, A. K. (1953): A Stability Index for Thunderstorm Forecast. *B. Am. Meteorol. Soc.*, **34**, 350–352.

Weisman, M. L. and Rotunno, R. (2000): The Use of Vertical Wind Shear versus Helicity in Interpreting Supercell Dynamics. *J. Atmos. Sci.,* **57**, 1452–1478.

Wilson J. W. and Schreiber, W. E. (1986): Initiation of Convective Storms at Radar-Observed Boundary-Layer Convergence Lines. *Mon. Weather Rev.*, **114**, 2516–2536.

Ziegler, C. L., Rasmussen, E. N., and Shepherd, T. R. (2001): The Evolution of Low-Level Rotation in the 29 May Newcastle-Graham, Texas, Storm Complex during VORTEX. *Mon. Weather Rev.*, **129**, 1339–1368.

SAŽETAK

Uzroci razvoja superćelije i tornadogeneze 30. kolovoza 2003.

Ivana Stiperski

U poslijepodnevnim satima 30. kolovoza 2003. u sjevero-zapadnom dijelu Hrvatske zabilježen je prolazak superćelije uz koji je bila vezana i pojava tornadogeneze. Iz radarskih je i satelitskih slika vidljivo da se ćelija formirala u Sloveniji te da se nakon prelaska u Hrvatsku uslijed povoljnog polja vjetra (velike vrijednosti *SREH* i vertikalnog smicanja vjetra) razvila u superćeliju. Procesi prisile bili su primarno mezoskalni. Temperaturni greben i uz njega vezana baroklina granica uočena na području Hrvatske i Slovenije prema istraživanjima provedenim u SAD-u karakteristični su za pojavu i jačanje superćelija. Dodatni izvori prisile bili su konvergencija vezana uz lijevi ulazni kvadrant mlazne struje i granicu izlaznog toka konvekcije vezane uz prolazak hladne fronte u noćnim satima. Nekoliko indeksa stabilnosti i indeksa olujnog vremena je testirano za ovaj slučaj konvekcije s izostankom makroskalne prisile te je nađeno da većinom nisu odgovarali stvarnom intenzitetu konvekcije.

Ključne riječi: superćelija, baroklina granica

Author's address: Ivana Stiperski, Meteorological and Hydrological Service, Zagreb, Croatia, Grič 3, 01/4565 721, e-mail: stiperski@cirus.dhz.hr